# Direct Synthesis of N-Heterocyclic Carbene-Stabilized Copper Nanoparticles from a N-Heterocyclic Carbene-Borane

Xavier Frogneux, Laura Hippolyte, Dimitri Mercier, David Portehault,
Corinne Chanéac, Clément Sanchez, Philippe Marcus, François Ribot, Louis
Fensterbank, Sophie Carenco

# Direct Synthesis of *N*-Heterocyclic Carbene-Stabilized Copper Nanoparticles from a *N*-Heterocyclic Carbene-Borane

Xavier Frogneux,[a],[b] Laura Hippolyte,[a],[c] Dimitri Mercier,[d] David Portehault,[a] Corinne Chanéac,[a] Clément Sanchez,[a],[b] Philippe Marcus,[d] François Ribot,*[a] Louis Fensterbank,*[c] Sophie Carenco*[a]

**Abstract:** *N*-Heterocyclic carbene(NHC)-stabilized copper nanoparticles are synthesized using a NHC-borane and mesitylcopper(I) in thermal conditions (refluxing toluene for 2.5 h). Nanoparticles (NPs) with a size distribution of 11.6 ± 1.8 nm were obtained. The interaction between Cu NPs and NHC ligands was probed by XPS, showing the covalent binding of the NHC to the surface of the nanoparticles. Mechanistic studies suggest that the NHC-borane plays two roles: contributing to the reduction of [CuMes]$_2$ to release Cu$^0$ species and providing NHC ligands to stabilize the copper nanoparticles.

## Introduction

*N*-Heterocyclic carbenes (NHCs) are often considered as a versatile family of compounds in modern chemistry and accordingly they have attracted the attention of various fields since the early 90s.[1,2] The taming of these compounds has unlocked a wide range of new applications from academia to industry, in organometallic chemistry, organocatalysis, surface chemistry and nanoparticles synthesis.[3,4] Although metallic nanoparticles display a promising range of applications, depending on the physical and chemical properties of the metal, examples of NHC-stabilized nanoparticles are still limited to few metals (Scheme 1, left).[4,5] Common strategies for their preparation rely either on the reduction of an organometallic precursor (isolated or generated *in situ*)[6–11] or by ligand exchange.[11–13] In spite of numerous works concerning their syntheses and applications,[14] copper nanoparticles are still challenging to prepare as a colloidal solution, resistant to aggregation over time, and featuring a metallic surface that is not oxidized nor hydroxylated, as long as it is kept under inert atmosphere.[15] Their stabilization with NHC has only been mentioned very recently, when NHCs were used as additional ligands on supported pre-formed nanoparticles to tune the catalytic activity for the hydrogenation of alkynes.[16,17] Before this recent work, the interaction of copper surfaces with NHC was mostly probed on self-assembled monolayers onto flat surfaces,[18,19] and also on supported Cu nanoparticles post-grafted with IMes NHC (1,3-bis(2,4,6-trimethylphenyl)-1,3-dihydro-2H-imidazol-2-ylidene).[17]

Because NHC-borane adducts combine both the potential roles of stabilizing ligand source and reducing agent,[20] we envisioned them as good candidates for the synthesis of NHC-stabilized copper nanoparticles.
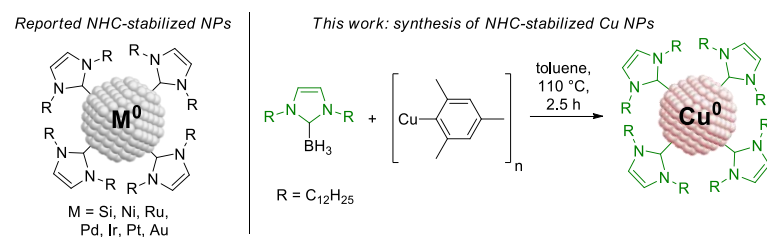


**Scheme 1.** (Left) Metal(loid) nanoparticles stabilized by NHC.[4] (Right) Proposed synthetic pathway using NHC-BH$_3$ adducts for the direct formation of copper nanoparticles stabilized by NHC.

## Results and Discussion

Previous works dealing with the synthesis of NHC-capped Au NPs showed the superior stabilization of nanoparticles with long alkyl chains (*n*-C$_{12}$H$_{25}$ or *n*-C$_{14}$H$_{29}$) on the NHC compared to shorter analogs.[6,11,13,21] Thus, we started our investigations using a NHC-borane with *n*-C$_{12}$H$_{25}$ aliphatic chains on the N atoms of the NHC core. [CuMes]$_n$ was previously used for the synthesis of colloidal copper nanoparticles.[22–27] In this study, the generation of copper nanoparticles was performed under inert atmosphere, using a solution of [CuMes]$_n$ in toluene, to which the NHC-BH$_3$ was added (1 to 5 equiv.). The solution was then heated at toluene reflux for 2.5 h, leading to a deep red suspension (Scheme 1, right). In contact with air, the final red suspension of nanoparticles was quickly oxidized, and took a blue color.

In order to narrow the size distribution of the nanoparticles, reaction conditions were screened (metal/NHC-borane ratio and concentration (see ESI, Table S1-2, Figure S1). A concentration of 100 mM for the Cu precursor and a 1:3 ratio of [CuMes]$_n$ to

[a] Dr. X. Frogneux, Dr. L. Hippolyte, Dr. D. Portehault, Pr. C. Chanéac, Pr. C. Sanchez, Dr. F. Ribot, Dr. S. Carenco
Sorbonne Université, CNRS, Collège de France, Laboratoire de Chimie de la Matière Condensée de Paris,
4 Place Jussieu, F-75005 Paris, France
E-mail: sophie.carenco@sorbonne-universite.fr;
francois.ribot@sorbonne-universite.fr

[b] Dr. X. Frogneux, Pr. C. Sanchez
Collège de France, PSL University, CNRS, Laboratoire de Chimie de la Matière Condensée de Paris,
11 Place Marcelin Berthelot, F-75005 Paris, France

[c] Dr. L. Hippolyte, Pr. L. Fensterbank
Sorbonne Université, CNRS, Institut Parisien de Chimie Moléculaire,
4 place Jussieu, 75252 Paris cedex 05, France
E-mail: louis.fensterbank@sorbonne-universite.fr

[d] Dr. D. Mercier, Pr. P. Marcus
ChimieParisTech, CNRS, PSL Research University, Institut de Recherche de Chimie Paris, Physical Chemistry of Surfaces Group,
F-75005 Paris, France

NHC-BH$_3$ were selected as the best conditions to obtain copper nanoparticles. The nanoparticles were isolated by centrifugation and washed under inert atmosphere, to remove any soluble molecular complexes or clusters. Transmission electron microscopy (TEM) indicated a size distribution of 11.6 ± 1.8 nm in diameter (Figure 1A).
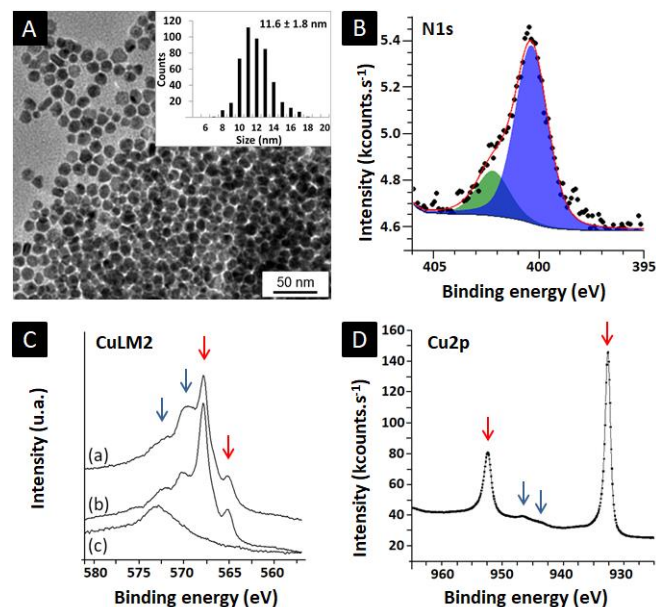


**Figure 1.** (A) TEM and size distribution of the isolated NPs (B) N1s XPS spectrum of Cu NPs and decomposition: blue = resulting from a covalent bonding; green = resulting from imidazolium contamination (C) CuLM2 Auger spectra of (a) Cu NPs, (b) bulk metallic copper reference and (c) [CuMes]$_n$ (D) Cu2p XPS spectrum

Due to the very high oxygen-sensitivity of these copper nanoparticles, we were unable to characterize their surfaces with routine TGA and IR analyses. We instead used X-ray photoelectron spectroscopy (XPS) to probe the surface species, without exposing the powder to air.[28] XPS measurements also give access to the Auger contributions of copper. XPS was performed on Cu NPs powder, NHC-BH$_3$ precursor and [CuMes]$_n$ (Figure 1B-D).

We first confirmed that copper was essentially in a metallic state in the Cu NPs powder. Figure 1C presents the CuLM2 Auger spectra obtained for the Cu NPs (a). Because of the intrinsically complex shape of Auger Cu spectra, it was compared to a bulk metallic copper reference (b) and the [CuMes]$_n$ precursor (c). Spectrum (a) of the Cu NPs presents the same four main transitions than the reference Cu metal (the two major ones are indicated by red arrows), clearly indicating the metallic character of the Cu NPs. Under the blue arrows are mostly contributions from the metallic copper, but also another contribution, as their intensity in spectrum (a) is higher than in spectrum (b). The presence of the [CuMes]$_n$ precursor can be totally excluded by

comparison with reference spectrum (c). In order to further identify the unknown contribution, the Cu2p photopeaks were analyzed (Figure 1D). They present two characteristic Cu2p$_{3/2}$ and Cu2p$_{1/2}$ components of metallic copper at 932.6 and 952.3 eV, respectively (Figure 1D, red arrows). This confirms the metallic character of copper as observed on the CuLM2 Auger spectrum, according to the work of Biesinger.[29] The presence of two weak peaks at 944 and 947 eV indicates electronically depleted copper centers (Figure 1D, blue arrows), and could be correlated with the additional contribution observed on the Auger peaks.

We propose that these weak transitions are related with the surface copper atoms that interact with the NHC ligand. In order to verify this hypothesis, we analyzed the C1s and N1s regions.

The C1s photopeak was dominated by the alkyl chain signal, supposedly from the NHC, preventing the detection of the characteristic component of the C–M covalent bond (see ESI, Figure S2A). However, the N1s photopeak clearly shows two distinct components, characteristic of specific chemical environments (Figure 1B). The major component at 400.3 eV was already observed in a previous study about NHC-stabilized Au NPs and is characteristic of the covalent binding of the NHC ligand to the metal nanoparticle through its N-C-N carbon.[21] In the present case, it was thus attributed to covalent binding of the NHC to the metal copper nanoparticles. We suggest that the surface Cu atoms bound to the NHC, rather than copper oxides/hydroxide impurity, are responsible for the additional components observed on CuLM2 Auger peak and Cu2p peaks, because the reaction and analysis were performed under oxygen-free conditions. The atomic composition estimated from XPS gives a NHC/Cu ratio of *ca* 1/20, corresponding to an apparent ratio of one NHC for two surface copper atoms. However, the precise determination of ligand coverage by XPS is not possible because the inelastic mean free path of photoelectrons, hence the depth of analysis, is lower than 5 nm: only a fraction of the nanoparticle is probed by XPS, which prevents a quantitative assessment. Based on a previous study on Au NPs prepared using an imidazolium precursor, the minor component (*ca* 20%) observed at 402.4 eV in the N1s region was tentatively attributed to imidazolium species contamination.[21] Indeed, the [CuMes]$_n$ commercial precursor contains significant amounts of Cl and Br impurities from its synthesis[30] (1% and 1.9% *vs*. Cu in mass respectively) which remains in the reaction medium and are precipitated with the nanoparticles. Because of the presence of Br impurity, the B1s region of XPS could not be interpreted, due to the overlap of B1s and Br3p peaks (see ESI, figure S2B).

Altogether, we can now provide a fairly complete description of the Cu NPs nanoparticles: these are metallic and exhibit NHC ligands at their surface as the major stabilizing species. NHC comes from the dissociation of the NHC-borane into NHC and

BH$_3$ (likely liberated in the gas phase as B$_2$H$_6$) in the presence of the copper surface, as schematized on Scheme 2 (bottom part). One central question remained: what is the pathway to form the Cu$^0$ species from [CuMes]$_n$? In order to answer this, the early stages of the nanoparticles formation were investigated.

First, we monitored by $^1$H{$^{11}$B} NMR and $^{11}$B NMR in toluene-$d_8$ the reaction, as performed above, between [CuMes]$_n$ and NHC-BH$_3$ (3 equiv.). The $^1$H{$^{11}$B} NMR and $^{11}$B NMR in toluene-$d_8$. The $^1$H{$^{11}$B} NMR spectrum of the crude revealed that all the initial [CuMes]$_n$ had reacted after 2.5 h at reflux. However, 90% of the initial NHC-BH$_3$ remained unreacted while the other 10% were converted into the NHC-BH$_2$Mes adduct (as evaluated by comparing the $^{11}$B NMR spectra of the mixture before and after heating). The latter species was identified from the triplet at -27.8 ppm in $^{11}$B NMR, and from singlets at 6.91 ppm (Ar-*H*, 2H), 2.83 ppm (MesB*H$_2$*-NHC, 2H), 2.46 ppm (o-C*H$_3$*, 6H) and 2.33 ppm (p-C*H$_3$*, 3H) in $^1$H{$^{11}$B} NMR (see ESI, Figure S3-5). It is worth noting that refluxing NHC-BH$_3$ in toluene does not alter it at all, as seen by $^1$H and $^{11}$B NMR. Mesitylene was also identified as a side-product (singlets at 6.65 ppm (Ar-*H*, 3H) and 2.13 ppm (–C*H$_3$*, 9H)). Surprisingly, in this reaction, less than one hydride per Cu atom was required for a complete reaction of the Cu precursor. This means that NHC-BH$_3$ did not act as a stoichiometric reactant for the reduction of Cu$^I$ species into Cu$^0$. Hence, the hydridic character of the NHC-BH$_3$ does not seem to be involved in the main pathway leading to Cu$^0$ species.

We investigated more in depth the reaction mechanism using complementary experiments. In the first one, [CuMes]$_n$ was heated at 110 °C for 2.5 h in the absence of NHC-BH$_3$. This resulted in the conversion of most of the [CuMes]$_5$ into [CuMes]$_2$,[31] with only traces of degradation products (see ESI, Figure S6). By TEM, few small and ill-defined nano-objects were observed, probably resulting from the degradation of the sensitive copper precursor (Figure S8B). This indicated that NHC-BH$_3$ was required for the complete transformation of [CuMes]$_n$ into copper nanoparticles.

NHC-boranes are known to form NHC-boryl radicals in the presence of a radical initiator.[32–34] In a second experiment, the possibility of a radical mechanism was thus explored using TEMPO as a radical scavenger. In the presence of 2 equiv. of TEMPO *vs.* Cu and 3 equiv. of NHC-BH$_3$ *vs.* Cu in the reaction medium, [CuMes]$_n$ only partially reacted after 2.5 h, leading to the formation of nanoparticles and mesitylene. However, NHC-BH$_2$Mes was not detected anymore by NMR (see ESI, Figure S6-7). Interestingly, the nanoparticles featured the same morphologies as for the experiment with a 1:1 ratio between [CuMes]$_n$ and NHC-BH$_3$ (Figure S8D). This was highly suggestive that the 2 equiv. of TEMPO are able to scavenge 2 equiv. of NHC-boryl radical. Besides, NHC was essential to the stabilization of the nanoparticles, as the reaction conducted with 2 equiv. of TEMPO but without NHC-BH$_3$ produced few nanoparticles with ill-defined shapes (Figure S6, S8C). While NMR was not sensitive nor discriminative enough, HRMS was able to highlight new species: using 4 equiv. of TEMPO , the NHC-boryl radical – TEMPO adduct could be detected by HRMS analysis ([C$_{36}$H$_{72}$N$_3$OB+H$^+$], calcd: 574.58412, found: 574.58384) (Figure S9-12).[35] Therefore, the presence of a radical species (TEMPO) affected the ability of the NHC-borane to react with the copper precursor and to stabilize the nanoparticles.
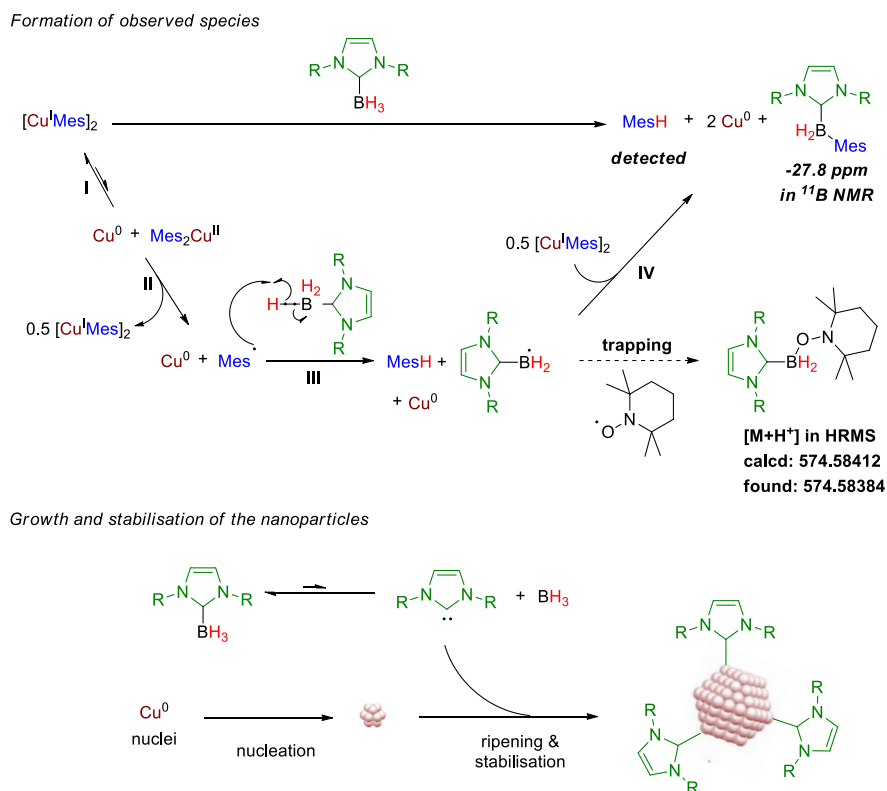
**Scheme 2.** (Top) Proposed mechanistic pathway for the formation of Cu⁰ species and observed side-products. (Bottom) Proposed pathway from Cu⁰ species to NHC-stabilized nanoparticles.

In order to reconcile all these observations, we propose the radical pathway depicted in Scheme 2: after dismutation of $[CuMes]_2$ into Cu⁰ and Cu²⁺ species (step **I**),[36–38] the later undergoes one Cu-C homoleptic bond cleavage, leading to the generation of mesityl radical and regeneration of a mesitylcopper(I) complex (step **II**).[39] This mesityl radical is keen to perform the hydrogen abstraction from the initial NHC-BH₃,[40] forming a NHC-boryl radical and mesitylene as byproduct (step **III**). Reaction of the NHC-boryl radical with mesitylcopper(I) complex, either by single-electron transfer or by hemolytic substitution, would lead to the formation of the NHC-BH₂Mes adduct and Cu⁰ (step **IV**).[43] In the presence of TEMPO initially introduced in the reaction medium, the NHC-boryl adduct was successfully trapped and detected by HRMS, which is strongly supportive of the formation of the NHC-boryl radical. While this mechanism rationalizes both formations of the NHC-mesitylborane adduct and mesitylene, the fact that the final experimental ratio (3:7) between these byproducts is not 1:1 seems to indicate that the mesityl radical reacted with another hydrogen source or that a second pathway could also be responsible for the formation of nanoparticles. Once copper(0) species are generated in solution, they aggregate into nanoparticles, which are stabilized by NHC-ligands, originating from the dissociation of NHC-borane adducts at 110 °C possibly catalyzed by the nascent Cu⁰ nanoparticles. Few NHCs ligands

are actually required to stabilize the copper NPs. Indeed, with a diameter of 11.6 nm, they have *ca.* 10-15% of their Cu atoms on the surface. With an initial NHC-BH₃/Cu ratio of 3 and assuming one NHC ligand for two surface copper atoms, only 1 to 3% of the initially introduced NHC-BH₃ has to be converted to NHC, a minute amount, the disappearance of which is difficult to probe by ¹H or ¹¹B NMR.

## Conclusions

As a conclusion, we reported here the first example of colloidal synthesis of NHC-stabilized copper nanoparticles. These were straightforwardly prepared using NHC-boranes as a NHC source and mesitylcopper(I) as metallic precursor. The role of the borane in NHC-BH₃ seems to be the trapping of the mesityl radical, which releases Cu⁰ species. The identification of the side-products of the reaction suggests that the formation of Cu⁰ species involves a radical pathway. The nature of the metal-ligand bond at the nanoparticles surface has been characterized by XPS and showed that the interaction between the nanoparticles and the carbene moiety is covalent. Functional copper nanoparticles are now reachable from this one-step synthetic route thanks to the rich modularity of NHCs. Furthermore, we expect this methodology to be suitable for the

synthesis of NHC-stabilized nanoparticles of other transition metals.

## Experimental Section

Unless stated otherwise, all syntheses and procedures were carried under inert gas (N$_2$ or Ar) using a glovebox (H$_2$O: ≤ 0.5 ppm, O$_2$: ≤ 0.5 ppm) or a Schlenk line in oven dried glassware.

**1,3-didodecylimidazolium bromide** (prepared according to a modified literature procedure[41]): imidazole (500 mg, 7.4 mmol) was dissolved in THF (5 mL) and was added to a solution of sodium hydride (60% w/w, 324 mg, 8.1 mmol) in THF (5 mL) at 0 °C. The ice bath was removed and the mixture was stirred for 1 h at room temperature. After dropwise addition of 1-bromododecane (3.5 mL, 14.7 mmol), the mixture was stirred at room temperature for at least 1 h before being heated at 70 °C until completion of the reaction (at least 24 h). Upon completion, the mixture was evaporated under reduced pressure. The residue was dissolved in dichloromethane and filtered. The filtrate was evaporated under reduced pressure, and dissolved in diethyl ether and left at 4 °C for 2 h. After filtration, the precipitate was dried in vacuo to give the product as a white powder (2.75 g, 5.7 mmol). Yield: 77%

$^1$H NMR (400 MHz, CDCl$_3$): δ 10.88 (t, $J$=1.3 Hz, 1H, N=C$H$-N), 7.20 (d, $J$=1.3 Hz, 2H, N-C$H$=C$H$-N), 4.36 (t, $J$=7.4 Hz, 4H, N-C$H_2$-),), 1.92 (quint, $J$=7.4 Hz, 4H, N-CH$_2$-C$H_2$-C), 1.35-1.25 (m, 36H, aliphatic chain), 0.88 (t, $J$=6.5 Hz, 6H, -C$H_3$). $^{13}$C{$^1$H} NMR (101 MHz, CDCl$_3$): δ 137.70, 121.78, 50.29, 32.00, 30.44, 29.70, 29.60, 29.49, 29.43, 29.11, 26.37, 22.78, 14.22. HRMS calculated for C$_{27}$H$_{53}$N$_2$$^+$: $m/z$: 405.4203, found: 405.4197.

**1,3-didodecylimidazol-2-ylidene borane (NHC-BH$_3$)** (prepared according to a modified literature procedure[42]): 1,3-didodecylimidazolium bromide (2 g, 4.1 mmol) was dissolved in THF (20 mL) and cooled to -78 °C. A solution of potassium bis(trimethylsilyl)amide (1 M in THF) (4.3 mL, 4.3 mmol) was added. The mixture was stirred at -78 °C for 1 h before addition of a solution of BH$_3$·THF (1 M in THF) (4.1 mL, 4.1 mmol). The cooling bath was removed and the reaction was stirred overnight at room temperature. The solvent was removed under reduced pressure. The residue was dissolved in dichloromethane and filtered. The filtrate was evaporated under reduced pressure. The resulting yellow oil was purified by column chromatography over silica gel (eluent mixture: pentane/dichloromethane, 55/45) to give the pure product as a white powder (750 mg, 1.8 mmol). Yield: 44%

$^1$H NMR (400 MHz, CDCl$_3$): δ 6.79 (s, 2H, N-C$H$=C$H$-N), 4.09 (t, $J$=7.6 Hz, 4H, N-C$H_2$-), 1.77 (quint, $J$=7.6 Hz, 4H, N-CH$_2$-C$H_2$-C), 1.35-1.15 (m, 36H, aliphatic chain), 0.88 (t, $J$=6.5 Hz, 6H, -C$H_3$). $^{13}$C{$^1$H} NMR (101 MHz, CDCl$_3$): δ 170.16, 118.80, 48.84, 32.04, 30.26, 29.75, 29.68, 29.62, 29.47, 29.32, 26.65, 22.81, 14.24. $^{11}$B NMR (96 MHz, CDCl$_3$): δ -37.3 (q, $J$=85.7 Hz, $B$H$_3$). HRMS calculated for C$_{27}$H$_{52}$N$_2$BH$_3$Na$^+$: $m/z$: 441.4356, found: 441.4347.

**Cu NPs synthesis procedure** for NPs presented in Figure 1: in a Schlenk tube, 0.3 mL of a 100 mM solution of [CuMes]$_n$ in toluene (18.3 mg, 0.1 mmol in 1 mL of toluene) were mixed with 0.9 mL of a 100 mM solution of NHC-BH$_3$ in toluene (43.3 mg, 0.1 mmol in 1 mL of toluene). The resulting solution (1.2 mL total) was stirred at toluene reflux for 2.5 h. After that time, an aliquot was taken and analyzed by TEM. Additional synthetic details are in Supplementary Information.

For NMR analysis, the reaction was prepared as following: in a glovebox, an air-tight NMR tube was successively charged with [CuMes]$_n$ (5.5 mg, 0.03 mmol), NHC-BH$_3$ (39 mg, 0.09 mmol) and 600 μL of toluene-$d_8$. The NMR tube was then heated in an oil bath at reflux for 2.5 h (N.B.: the solution rapidly turned deep red after few minutes of heating). The starting mixture and the crude obtained after heating were analyzed by $^1$H, $^1$H{$^{11}$B} and $^{11}$B NMR.

[1]     A. J. Arduengo, R. L. Harlow, M. Kline, *J. Am. Chem. Soc.* **1991**, *113*, 361–363.

[2]     M. N. Hopkinson, C. Richter, M. Schedler, F. Glorius, *Nature* **2014**, *510*, 485–496.

[3]     D. M. Flanigan, F. Romanov-Michailidis, N. A. White, T. Rovis, *Chem. Rev.* **2015**, *115*, 9307–9387.

[4]     A. V Zhukhovitskiy, M. J. MacLeod, J. A. Johnson, *Chem. Rev.* **2015**, *115*, 11503–11532.

[5]     S. Engel, E. Fritz, B. J. Ravoo, *Chem. Soc. Rev.* **2017**, 2057–2075.

[6]     J. Vignolle, T. D. Tilley, *Chem. Commun.* **2009**, 7230.

[7]     P. Lara, O. Rivada-Wheelaghan, S. Conejero, R. Poteau, K. Philippot, B. Chaudret, *Angew. Chem. Int. Ed.* **2011**, *50*, 12080–12084.

[8]     X. Ling, N. Schaeffer, S. Roland, M. Pileni, *Langmuir* **2013**, *29*, 12647–12656.

[9]     E. A. Baquero, S. Tricard, J. C. Flores, E. de Jesus, B. Chaudret, *Angew. Chem. Int. Ed.* **2014**, *53*, 13220–13224.

[10]    M. D. de los Bernardos, S. Pérez-Rodríguez, A. Gual, C. Claver, C. Godard, *Chem. Commun.* **2017**, *53*, 7894–7897.

[11]    R. W. Y. Man, C.-H. Li, M. W. A. MacLean, O. V Zenkina, M. T. Zamora, L. N. Saunders, A. Rousina-Webb, M. Nambo, C. M. Crudden, *J. Am. Chem. Soc.* **2018**, 1576–1579.

[12]    E. C. Hurst, K. Wilson, I. J. S. Fairlamb, V. Chechik, *New J. Chem.*

**2009**, *33*, 1837–1840.

[13]   C. Richter, K. Schaepe, F. Glorius, B. J. Ravoo, *Chem. Commun.* **2014**, *50*, 3204–3207.

[14]   M. B. Gawande, A. Goswami, F.-X. Felpin, T. Asefa, X. Huang, R. Silva, X. Zou, R. Zboril, R. S. Varma, *Chem. Rev.* **2016**, *116*, 3722–3811.

[15]   V. A. Online, D. Adner, M. Korb, S. Schulze, M. Hietschold, H. Lang, *Chem. Commun.* **2013**, *49*, 6855–6857.

[16]   N. Kaeffer, H.-J. Liu, H.-K. Lo, A. Fedorov, C. Copéret, *Chem. Sci.* **2018**, *4*, 5366–5371.

[17]   N. Kaeffer, K. Larmier, A. Fedorov, C. Copéret, *J. Catal.* **2018**, *364*, 437–445.

[18]   C. R. Larrea, C. J. Baddeley, M. R. Narouz, N. J. Mosey, J. H. Horton, C. M. Crudden, *ChemPhysChem* **2017**, *18*, 3536–3539.

[19]   L. Jiang, B. Zhang, G. Médard, A. P. Seitsonen, F. Haag, F. Allegretti, J. Reichert, B. Kuster, J. V. Barth, A. C. Papageorgiou, *Chem. Sci.* **2017**, *8*, 8301–8308.

[20]   D. P. Curran, A. Solovyev, M. Makhlouf Brahmi, L. Fensterbank, M. Malacria, E. Lacôte, *Angew. Chem. Int. Ed.* **2011**, *50*, 10294–10317.

[21]   N. Bridonneau, L. Hippolyte, D. Mercier, D. Portehault, M. Desage-El Murr, P. Marcus, L. Fensterbank, C. Chanéac, F. Ribot, *Dalt. Trans.* **2018**, *47*, 6850–6859.

[22]   M. Stollenz, F. Meyer, *Organometallics* **2012**, *31*, 7708–7727.

[23]   C. Barrière, G. Alcaraz, O. Margeat, P. Fau, J. B. Quoirin, C. Anceau, B. Chaudret, *J. Mater. Chem.* **2008**, *18*, 3084.

[24]   C. Barrière, K. Piettre, V. Latour, O. Margeat, C.-O. Turrin, B. Chaudret, P. Fau, *J. Mater. Chem.* **2012**, *22*, 2279.

[25]   S. D. Bunge, T. J. Boyle, T. J. Headley, *Nano Lett.* **2003**, *3*, 901–905.

[26]   A. Fedorov, H. Liu, H. Lo, C. Copéret, *J. Am. Chem. Soc.* **2016**, *138*, 6–11.

[27]   S. D. Pike, E. R. White, A. Regoutz, N. Sammy, D. J. Payne, C. K. Williams, M. S. P. Shaffer, *ACS Nano* **2017**, *11*, 2714–2723.

[28]   J. Świątowska-Mrowiecka, V. Maurice, S. Zanna, L. Klein, P. Marcus, *Electrochim. Acta* **2007**, *52*, 5644–5653.

[29]   M. C. Biesinger, *Surf. Interface Anal.* **2017**, *49*, 1325–1334.

[30]   T. Tsuda, T. Yazawa, K. Watanabe, T. Fujii, T. Saegusa, *J. Org. Chem.* **1981**, *46*, 192–194.

[31]   C. Floriani, E. M. Meyer, S. Gambarotta, A. Chiesi-Villa, C. Guastini, *Organometallics* **1989**, *8*, 1067–1079.

[32]   S. H. Ueng, M. M. Brahmi, É. Derat, L. Fensterbank, E. Lacôte, M. Malacria, D. P. Curran, *J. Am. Chem. Soc.* **2008**, *130*, 10082–10083.

[33]   S. H. Ueng, A. Solovyev, X. Yuan, S. J. Geib, L. Fensterbank, E. Lacôte, M. Malacria, M. Newcomb, J. C. Walton, D. P. Curran, *J. Am. Chem. Soc.* **2009**, *131*, 11256–11262.

[34]   M. A. Tehfe, M. M. Brahmi, J. P. Fouassier, D. P. Curran, M. Malacria, L. Fensterbank, E. Lacôte, J. Lalevée, *Macromolecules* **2010**, *43*, 2261–2267.

[35]   N. Zhou, X. A. Yuan, Y. Zhao, J. Xie, C. Zhu, *Angew. Chem. Int. Ed.* **2018**, *57*, 3990–3994.

[36]   F. Fenwick, *J. Am. Chem. Soc.* **1926**, *385*, 860–870.

[37]   D. Ferri, R. Palombari, *J. Inorg. Nucl. Chem.* **1979**, *42*, 593–598.

[38]   B. M. Rosen, X. Jiang, C. J. Wilson, N. G. A. H. Nguyen, M. J. Monteiro, V. Percec, *J. Polym. Sci. A* **2009**, *47*, 5606–5628.

[39]   J. T. B. H. Jastrzebski, G. van Koten, in *Mod. Organocopper Chem.* (Ed.: N. Krause), Wiley-VCH Verlag GmbH, Weinheim, **2002**, pp. 1–44.

[40]   A. Solovyev, S. H. Ueng, J. Monot, L. Fensterbank, M. Malacria, E. Lacôte, D. P. Curran, *Org. Lett.* **2010**, *12*, 2998–3001.

[41]   S. V. Dzyuba, R. A. Bartsch, *Chem. Commun.* **2001**, *1*, 1466–1467.

[42]   J. C. Walton, M. M. Brahmi, L. Fensterbank, E. Lacôte, M. Malacria, Q. Chu, S.-H. Ueng, A. Solovyev, D. P. Curran, *J. Am. Chem. Soc.* **2010**, *132*, 2350–2358.

[43]   For a resembling formation of NHC borane-mesityl adduct in hte presence of MesMgBr, see: C. Aupic, A. A. Mohamed, C. Figliola, P. Nava, B. Tuccio, G. Chouraqui, J.-L. Parrain O. Chuzel, *Chem. Sci.* **2019**, *doi:*10.1039/c9sc01454c